## Title
Toroidal Alfvén eigenmode avalanches in NSTX

**Journal**
35th EPS Conference on Plasma Physics 2008, EPS 2008 - Europhysics Conference Abstracts, 32(3)

**ISBN**
9781622763351

**Authors**
Fredrickson, ED
Crocker, NA
Darrow, D
et al.

**Publication Date**
2008-12-01

*35th EPS Conference on Plasma Phys. Hersonissos, 9 - 13 June 2008 ECA Vol.**32D**, P-5.060 (2008)*

# Toroidal Alfvén Eigenmode Avalanches in NSTX

E. D. Fredrickson, N. A. Crocker[2], D. Darrow, N. N. Gorelenkov, W. W. Heidbrink[1], S. Kubota[2], F. M. Levinton[3], D. Liu[1], S. S. Medley, M. Podesta[1], H. Yuh[3], R. E. Bell

*Princeton Plasma Physics Laboratory, Princeton New Jersey 08543*
[1]*Univ. of Caliifornia., Irvine, CA 92697*
[2]*Univ. of California, Los Angeles, CA 90095*
[3]*Nova Photonics, Princeton, NJ 08543*

While single Toroidal Alfvén Eigenmodes (TAE) are not expected to cause substantial fast ion transport in ITER, multiple modes, particularly if they strongly interact, becoming non-linear as in an ´avalanche event´ [1], can affect ignition thresholds, redistribute beam-driven currents and damage PFCs. The TAE avalanche threshold has been measured on NSTX and the concomitant fast ion losses are studied.

At a threshold in beam beta roughly 30% higher than the threshold for TAE onset, the sequence of TAE bursts culminates in an avalanche; that is a very large burst, 5 to 10 times larger in amplitude, and with more visible modes. At this time, drops in the neutron rate of ≈ 10%, and spikes in $D_a$ emission are seen. Redistribution of low energy fast ions has also been seen with the Neutral Particle Analyzer (NPA) diagnostics.

The threshold for onset of TAE and TAE avalanches was studied by varying the beam voltage and power in a sequence of otherwise similar plasmas. Beginning below the threshold for TAE, with one neutral beam source at 65 kV, the plasmas are quiescent (Fig. 1a). An increase to two sources at 65 kV reaches the threshold for TAE onset (Fig. 1b). Finally, increasing one source voltage to 70 kV triggers avalanches and concomitant

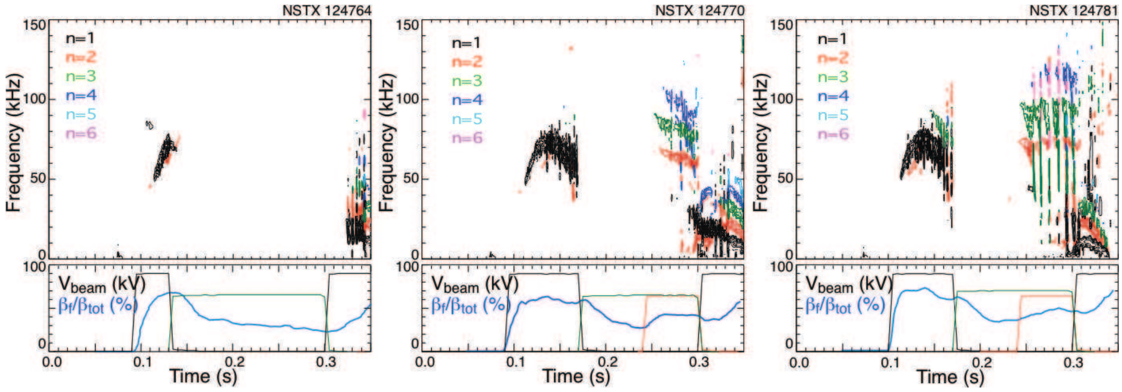

Fig. 1 Spectrograms of magnetic fluctuations in a plasma sequence illustrating a scan in $b_{fast}$; a) $b_{fast}$ below threshold for exciting TAE from 0.14 s to 0.32 s. b) $\beta_{fast}$ at threshold for exciting TAE after 0.25 s, c) $\beta_{fast}$ above threshold for exciting TAE avalanches after 0.26 s. Higher voltage beam periods, e.g., c) 0.1 to 0.17s and after 0.3s, are for MSE measurement of field pitch angle.

neutron drops (Fig. 1c).

Enhanced fast-ion losses are studied with multi-channel NPA diagnostics and fast neutron rate monitors. Evidence of fast-ion redistribution is also seen in the four-channel mid-plane NPA. In Fig. 2b is shown the energy resolved, time-dependant NPA spectrum at 60 cm tangency radius during the TAE avalanches. Of particular interest is that the redistribution extends down to energies at least as low as 30 keV, less than half the full energy of injection. Loss of fast ions is indicated by drops of ≈ 10% in the neutron rate at each avalanche event (Fig. 2c).

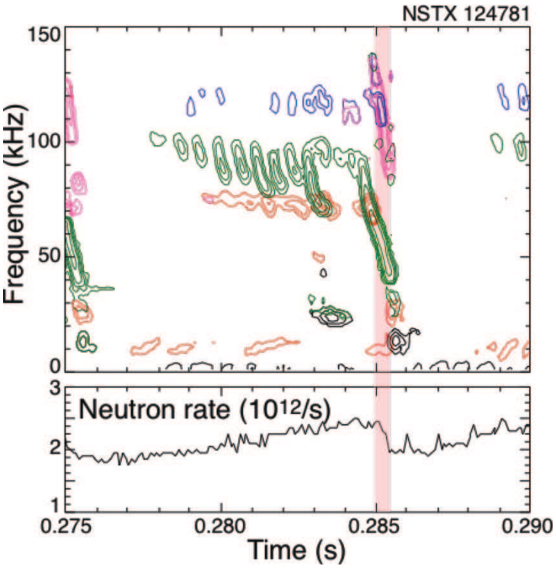

Fig. 3. a) Detail spectrogram of single avalanche cycle. Colors indicate toroidal mode numbers (black ´ 1, red ´ 2, green ´ 3, blue ´ 4, magenta ´ 6), b) neutron rate showing drop at avalanche.

The mode structure and fast ion transport are modeled with the NOVA and ORBIT codes. For input to these codes, the plasma equilibrium is reconstructed during the avalanching period using the equilibrium code, LRDFIT, which uses Motional Stark Effect (MSE) data to constrain the current profile. The MSE diagnostic relies on one 90 kV source, thus is not available during the avalanching period, but is acquired from 0.13 s to 0.17 s early in the discharge, and after 0.3 s later in the discharge. Further, a similar discharge was made where the 90 kV source was substituted for the two lower voltage sources, at nearly the same power. Comparison of the data from these shots suggests that the q-profile evolution was not strongly affected by the substitution of sources, and the q-profile evolution measured in the shot with a 90 kV beam is used for analysis.

The beam deposition model in TRANSP is used to model the fast-ion distribution function. As the target plasma was Helium, comparison of TRANSP predicted neutron rates with measured neutron rates gives little information on whether the calculated fast-ion distribution is being strongly modified by MHD as the Helium-Deuterium ratio is not independently measured, and thus can be adjusted to fit any measured neutron rate, within reason.

The use of Helium in the target plasma was motivated by the desire for peaked (L-mode) density profiles, needed for reflectometer measurements of the internal mode structure and amplitude. The internal mode structure and amplitude is measured with a five-channel, fixed-frequency reflectometer system. The five channels have cut-off density ranging from ≈ 1.2 x $10^{13}$/$cm^3$ up to ≈ 3.1 x $10^{13}$/$cm^3$. The target plasma density was chosen to provide measurements of the mode over most of the minor radius.

The NOVA simulations were done primarily for the plasma equilibrium conditions at the avalanche at 0.285 s shown in Fig. 1. The TAE activity began at ≈ 0.25 s in this shot, with the first avalanche at 0.258 s. The avalanching ended at 0.3 seconds, when a single 90 kV source was substituted for the 65 kV and 70 kV sources, although the character of the avalanches had been evolving. Qualitatively, TAE activity showed a weak shift towards higher toroidal mode numbers, n during the sequence of avalanches. The q-profile and density were still slowly evolving during this time, with $q_{min}$ dropping from about ≈ 1.4 at 0.26 s to ≈ 1.15 at 0.3 s and density increasing by about 10%. The q on axis, while less accurately known, showed a smaller decrease. This change in q-profile could affect the gap width on axis, affecting the stability of the TAE.

The NOVA code was used to find eigenmode solutions for the four dominant TAE modes seen in the avalanche at 0.285 s. The dominant mode was the n = 3 mode, accompanied by n = 2, n = 4, and n = 6 modes. The gap structure for the n = 3 mode is shown in Fig. 4a. With q(0) ≈ 1.5, the gap is fairly narrow on axis at this time. The Doppler-corrected local mode frequency in the plasma frame is shown in red, and the NOVA eigenmode frequency is indicated by the blue dashed line. Thus, the NOVA frequency is *consistent* with the observed mode frequency, but questions remain as to the affect of the sheared rotation on the eigenfunction shape and stability. NOVA has provisions to model some effects of sheared rotation which future work will address.

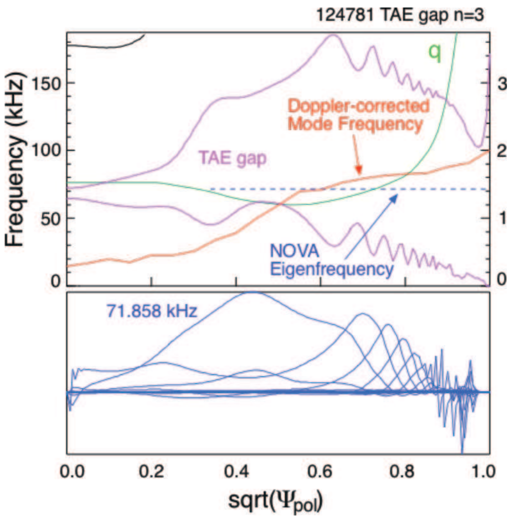

Fig 4. NOVA simulations for the n = 3 mode at 0.285s. a) Magenta curves show TAE gap, green curve shows the q-profile (axis on right), red curve shows the local, Doppler-corrected mode frequency (plasma frame), dashed blue line shows NOVA eigenfrequency, b) poloidal harmonics of the n = 3 mode at 72 kHz.

The comparison of the modeled reflectometer response for the NOVA n=3 eigenmode at 72 kHz with the experimental data is show in Figure 5. The phase extracted from the quadrature or heterodyne reflectometer data partially reflects an interferometric measurement of the density outside the cut-off layer, and the displacement of the cut-off layer itself. The reflectometer data is interpreted through comparison with a ´synthetic reflectometer diagnostic´ using the linear mode calculations from the NOVA code (Fig. 4b). For simplicity, the phase, simulated and measured, is represented as the displacement in the long-wavelength approximation (d-phase/$k_{vacuum}$). The eigenfunctions are relatively ´smooth´, so the five radial data points from the reflectometer array are sufficient to provide a good comparison.

We have identified and fully diagnosed plasmas with TAE avalanches on NSTX. As is predicted for ITER, the interaction of multiple modes greatly enhances the fast ion losses. The measurements of mode amplitude and radial profile can be used to benchmark NOVA and used in ORBIT to simulate fast ion losses.

Work supported by U.S. DOE Contracts DE-AC02-76CH03073, DE-FG03-99ER54527, DE-FG02-06ER54867, and DE-FG02-99ER54527.

**References**

[1] H. L. Berk, B. N. Breizman, M. Pekker, Phys. Plasmas **2**, 3007 (1995)

[2] E.D. Fredrickson, N N Gorelenkov, R E Bell, J E Menard, A L Roquemore, S. Kubota, N A Crocker, W Peebles, Nucl. Fusion **46**, s926 (2006).